Cellular Signalling 60 (2019) 100–113

Contents lists available at ScienceDirect

Cellular Signalling

journal homepage: www.elsevier.com/locate/cellsig

Transcriptional activation of SIRT6 *via* FKHRL1/FOXO3a inhibits the Warburg effect in glioblastoma cells

Zhen Dong[a,b,c,d], Xiaoxia Zhong[a,b,c,d], Qian Lei[a,b,c,d], Fei Chen[e,*], Hongjuan Cui[a,b,c,d,**]

[a] State Key Laboratory of Silkworm Genome Biology, Institute of Sericulture and Systems Biology, Southwest University, Beibei, Chongqing 400716, China
[b] Engineering Research Center for Cancer Biomedical and Translational Medicine, Southwest University, Beibei, Chongqing 400716, China
[c] Chongqing Engineering and Technology Research Center for Silk Biomaterials and Regenerative Medicine, Southwest University, Beibei, Chongqing 400716, China
[d] Cancer Center, Medical Research Institute, Southwest University, Beibei, Chongqing 400716, China
[e] Department of Pharmaceutical Sciences, Eugene Applebaum College of Pharmacy and Health Sciences, Wayne State University, Detroit, MI 48201, USA

ARTICLE INFO

Keywords:
FKHRL1
SIRT6
The Warburg effect
Aerobic glycolysis
Glioblastoma

ABSTRACT

Glioblastoma (GBM) is the most aggressive and malignant form of brain tumors. However, its molecular mechanisms of tumorigenesis and cancer development remains to elucidate. Here, we reported FKHRL1, also called as FOXO3a, was an anti-cancer factor that inhibited the Warburg effect in GBM. Clinical data analysis revealed that FKHRL1 expression was positively correlated with the prognosis of patients with GBM. FKHRL1 silencing promoted glycolysis and cell growth of HEB gliocytes. Besides, FKHRL1 expression was tightly correlated with the expression of SIRT6 and a cluster of glycolytic genes that controlling the Warburg effect in glioma samples. Interestingly, the expression of SIRT6 was reduced after FKHRL1 knockdown, while its expression was upregulated when FKHRL1 was overexpressed in human U251 GBM cell line. In addition, SIRT6 restoration recovered the upregulated aerobic glycolysis induced by FKHRL1 knockdown. Meanwhile, SIRT6 knockdown also rescued the decrease of glucose metabolism induced by FKHRL1 overexpression. Luciferase assay and chromatin immunoprecipitation (ChIP) assay revealed that FKHRL1 bound to the promoter region of SIRT6 and enhanced its expression. Both *in vitro* and *in vivo* experiments further confirmed that FKHRL1-SIRT6 axis played a pivotal role in cell metabolism and tumor growth. Our results indicate that FKHRL1-SIRT6 axis regulates cell metabolism and may provide clues for GBM treatment.

1. Introduction

Glioblastoma (GBM) is the most prevalent and malignant form of brain tumor. Most of patients die within 15 to 18 months after diagnosis, and only < 5% of patients survive > 5 years [1]. Despite the researchers are making efforts to determine the nature of GBM, only a little progress has been made to treat the GBM patients. The use of temozolomide, an alkylating cytotoxic agent, is a standard therapy for GBM. However, cancer cells in most patients achieve resistance against this drug [2,3]. Thus, there is dire need to develop some more effective drugs for the treatment of GBM.

Recently, reprogrammed cell metabolism has been recognized as a hallmark of cancer cells [4,5]. The Warburg effect, also named as aerobic glycolysis, is the most important alteration in cancer cell metabolism, which is characterized by excessive glycolysis and increase in glycolytic enzymes [6]. Besides, many factors, such as oncogenes (*e.g.* p53, c-Myc and K-Ras), essential signaling pathways (*e.g.* PI3K/Akt, LKB1/AMPK, HIF-1 signaling pathways) and epigenetic regulators (*e.g.* sirtuins) participate into the regulation of the Warburg effect [6–9]. Recently, many other factors have also been reported to involve in the regulation of the Warburg effect in GBM. For example, miR-143 inhibits glycolysis by directly targeting hexokinase 2 (HK2), thereby promoting cell differentiation of glioblastoma stem-like cells [10]. These factors can be therapeutic targets for GBM treatment. For example, inhibitors of the NAD(+) salvage enzyme nicotinamide phosphoribosyl-transferase (NAMPT) represent a novel metabolically targeted therapeutic strategy for MYC or MYCN-amplified GBM [11].

FKHRL1, also named as FKHR, FOXO3a and AFX, is an important member of DAF-16-like transcription factors, and plays a key role in the suppression of tumor by modulating cell cycle [12], DNA damage [13],

* Correspondence to: F. Chen, Department of Pharmaceutical Sciences, Eugene Applebaum College of Pharmacy and Health Sciences, Wayne State University, 259 Mack Avenue, Detroit, MI 48201, USA.
** Correspondence to: H. Cui, State Key Laboratory of Silkworm Genome Biology, Institute of Sericulture and Systems Biology, Southwest University, No.2 Tiansheng Road, Beibei District, Chongqing 400716, China.
E-mail addresses: fchen@wayne.edu (F. Chen), hcui@swu.edu.cn (H. Cui).

https://doi.org/10.1016/j.cellsig.2019.04.009
Received 18 December 2018; Received in revised form 16 April 2019; Accepted 16 April 2019
Available online 17 April 2019
0898-6568/

apoptosis [14–16], drug resistance [17] and epithelial-to-mesenchymal transition (EMT) [18] in cancers including GBM. Recently, it has been shown that FKHRL1 is an important regulator of cellular metabolism in cancer. For example, it can inhibit mitochondrial gene expression to regulate reactive oxygen metabolism in colon cancer [19]. However, its biological role has not been described previously in cell metabolism of GBM.

In the present study, we investigated the glycolysis regulatory role of FKHRL1 in GBM cells and determined its molecular mechanism in this process. Our study aimed to elucidate the regulatory mechanism of FKHRL1 in cellular metabolism and to provide clues for GBM treatment.

2. Materials and methods

2.1. Cell lines and reagents

U251 and U87 (ATCC, VA, USA) human GBM cell lines and HEB gliocytes were maintained in Dulbecco's modified Eagle's medium (DMEM, Life Technologies, Thermo Fisher, Shanghai, China) supplemented with 10% fetal bovine serum (FBS; Invitrogen, Thermo Fisher) and 1% Penicillin-Streptomycin (P/S, Invitrogen). 293FT cell line (ATCC) were maintained in DMEM supplemented with 10% FBS, 1% P/S, 1% MEM Non-Essential Amino Acids Solution (Invitrogen), 2 mM L-Glutamine (Invitrogen) and 1 mM Sodium Pyruvate (Invitrogen). 2-Deoxy-2-[(7-nitro-2,1,3-benzoxadiazol-4-yl)amino]-D-glucose (2-NBDG, N13195) was purchased from BD (BD Pharmingen, San Jose, CA, USA). LDH activity assay kit (MAK066), Dimethyl sulfoxide (DMSO, D2650) and 3-(4,5-dimethyl-2-thiazolyl)-2,5-diphenyl-2-H-tetrazolium bromide (MTT, M2128) were purchased from Sigma-Aldrich (Castle Hill, NSW, Australia).

2.2. Vector construction, transfection and infection

The RNAi target sites were designed and then synthesized by the Beijing Genomics Institute (BGI, Shenzhen, China) and were cloned into a lentiviral pLKO.1 vector. The target sequences of these sites were listed as below:

shFKHRL1#1: AATGTGACATGGAGTCCATTAT; shFKHRL1#2: GGACAATAGCAACAAGTATACC.

shSIRT6: AAGAATGTGCCAAGTGTAAGA.

Human full-length SIRT6 (GenBank: CR457200.1) cDNA was obtained by using PCR and was cloned into lentiviral pCDH-CMV-MCS-EF1-copGFP vector. The primers used as below:

SIRT6-F-(*Eco*RI): CCGGAATTCATGTCGGTGAATTACGCGGCGGC;

SIRT6-R -(BamHI): CGCGGATCCTTAACTGGGGACCGCCTTGG.

Letivirural vector construction, transfection and infection were employed as described previously [20]. HA-FKHRL1 WT plasmid was obtained from addgene (1787, Watertown, MA, USA) and FKHRL1 was constructed into the pCDH-CMV-MCS-EF1-copGFP vector.

2.3. Quantitative RT-PCR

RNA was extracted using Trizol (Takara, Dalian, China) according to the manufacturer's protocol and real-time quantitative PCR was performed as reported previously [21]. Results were calculated by the ΔΔCt method with β-actin expression as a control. The primers were listed as below:

fkhrl1, F: ACGTCTTCAGGTCCTCCTGTT, R: GGGGAAGCACCAAAGAAGAGAG;

sirt6, F: CTCGAAGTGGAGCTGGACC, R: TCCTCGGGGATCATGGAGTC;

glut1, F: TGTGTATGCCACCATTGGCT, R: CTAGCGCGATGGTCATGAGT;

glut4, F: GGACAGCCAGCCTACGCCACCATA, R: GGACAGCCAGCCTACGCCACCATA;

hk1, GCACGTTTGCACCATTGTCT, R: TTGTGGAAACGCCGGGAATA;

hk2, F: GAATGGGAAGTGGGGTGGAG, R: GAGGAGGATGCTCTCGTCCA;

hk3, F: TTCCCATGTAGGCAGCTTGG, R: ATGAGGCCTATCTCGCAACG,

gapdh, F: CTCTGCTCCTCCTGTTCGAC, R: GCGCCCAATACGACCAAATC;

pfk1, F: CTGCCCCTCATGGAATGTGT, R: ATACCGGGGGTCTGACATGA,

pkm2, F: AATGCAGTCCTGGATGGAGC, R: ACTGCAGCACTTGAAGGAGG;

ldh-a1, F: GGTCCTTGGGGAACATGGAG, R: TAGCCCAGGATGTGTAGCCT;

ldh-a2, F: AGCTGTTCCACTTAAGGCCC, R: AGGAATCGGGAATGCACGTC;

β-actin, F: CGTCTTCCCCTCCATCGTG, R: TCGATGGGGTACTTCAGGGT.

2.4. Flat plate clone formation test

Cell viability was determined by flat plate clone formation test on HEB cells. Briefly, 1000 scramble or FKHRL1-silenced cells were cultured in 6-well plate for 2 weeks. Then medium was removed and the cells was stained by 1% crystal violet solution (Beyotime) for 5 min and then washed gently by PBS solution. Afterwards, plates were scanned by an Epson scanner. Then 1 mL ethanol was added into each well of the plates, and shook for 5 min. The absorbance of 595 nm was detected by using a Thermo Fisher microplate reader.

2.5. Western blot

Western blot was performed as described previously [21]. The antibodies used in this study were listed as below: anti-FKHRL1/FOXO3a rabbit mAb (2497, Cell Signaling Technology, CST), anti-SIRT6 rabbit mAb (12486, CST) and anti-α-Tubulin Antibody (2144, CST).

2.6. MTT assay

1000 cells were cultured in the 96-well plates and MTT assay were described previously [22].

2.7. Glucose uptake assay

Cells were cultured in glucose-free DMEM (Invitrogen) with FBS and P/S for 2 h, and a fluorescent glucose analogue, 2-NBDG (100uM) dissolved in Kerbs-Ringer bicarbonate buffer (KRB buffer, 129 mM NaCl, 4.8 mM KCl, 5 mM $NaHCO_3$, 1.2 mM MgSO4, 2 mM $CaCl_2$, 10mMHEPES) was added into the medium and incubated for 2 h. Then the cells were collected and washed with KRB buffer, and the fluorescence of 2-NBDG in the cells was detected by using a BD Acurri C6 flow cytometer.

2.8. GO assay

Cells were cultured for 48 h, and then the glucose content in the medium was detected by a GO assay kit (GAGO20, Sigma-Aldrich) according to the manufacturer's protocol. Glucose consumption rates were calculated and normalized by cell numbers. For tumor samples, glucose content was normalized by protein content.

2.9. Lactate assay

Cells were cultured for 48 h, and then the lactate content in the medium was detected by a lactate assay kit (MAK064, Sigma-Aldrich) according to the manufacturer's protocol. The rate of lactate production was calculated and normalized by cell numbers. For tumor samples,

lactate content was normalized by protein content.

2.10. Lactate dehydrogenase (LDH) assay

Cells were cultured in DMEM for 48 h, and then the lactate dehydrogenase activity in cells was detected by a lactate dehydrogenase assay kit (MAK066, Sigma-Aldrich) according to the manufacturer's protocol. Relative LDH activities were calculated and normalized by cell number. For tumor samples, relative LDH activity was normalized by protein content.

2.11. Glycolytic stress flux test

Cells were plated into XF96 cell culture microplates and cultured for 24 h. Then the medium was changed into Seahorse basic DMEM with 2 mM glutamine, and the microplates were maintained in a non-CO_2 incubator at 37 °C for 60 min. The Seahorse XF glycolysis stress test was conducted as previously described [23]. 10 mM Glucose (Sangon, Shanghai), 1 μg/mL oligomycin (495455, Sigma-Aldrich) and 50 mM 2-deoxyglucose (2-DG, Sangon) at final concentration were used in this test.

2.12. Luciferase assay

The sequences of promoter regions were obtained from the genome DNA of 293FT cells by using PCR. The primers used were listed as below:

SIRT6-p-0.1k-*Nhe*I-F: CCGGCTAGCGCCCGGCTCACTCACTTTTTAG;

SIRT6-p-0.2k-NheI-F: CCGGCTAGCCTGCCTTGGCCTCCCAAAGT;

SIRT6-p-0.6k-NheI-F: CCGGCTAGCCTATCATCACTGGACTGATTTC AGTTTC;

SIRT6-p-1.2k-NheI-F: CCGGCTAGCGGGTAATAAGACACCCAACAG AGG;

SIRT6-p-*Xho*I-R: CCGCTCGAGGTAATGGTGACATGGTGTGGTTG;

SIRT6-p-N0.9k-NheI-F: CCGGCTAGCCTGGTCACATGTTTGTGTC CAC;

SIRT6-p-N0.9k-XhoI-R: CCGCTCGAGAAAGTTTCCCTTGTTGAGG CCG.

Wild-type and mutant Primer1 products were sent to Sangon to synthesize. All the sequences were constructed into pGL3 vector. Then pGL3 was transfected into 293FT cells and the luciferase assay was performed as previously described [24].

2.13. Chromatin immunoprecipitation (ChIP) assay

ChIP assays were performed in U251 cells by using the EZ CHIP™ kit as according to the manufacturer's protocol. Primers used in the present study were given below: SIRT6-p-F1: AAGACAATCCGTGGGCTTGG; SIRT6-p-R1: GAGCTACCCAGGTACCCTG. SIRT6-p-F2: TGGCTAGGACT CAGCACG; SIRT6-p-R2: TAGGGGAGGAAGGAGGTGG. The antibodies used were as followed: anti-FKHRL1 antibody (ab12162, Abcam, Cambridge, MA, USA), anti-RNA polymerase II CTD repeat YSPTSPS (phospho S5) antibody (ab5131, Abcam, Shanghai, China), histone H3ac (pan-acetyl) antibody (pAb) (39139, Active Motif, Shanghai, China) and normal rabbit IgG (Beyotime, Jiangsu, China).

2.14. Tumor xenografts

A total of 12 one-month-old female mice (BALA/c-nu, Beijing Huafukang Bioscience Co. Inc., China) were purchased and housed in the independent ventilation cages (IVCs) in a specific-pathogen-free (SPF) room to acclimate for about 10 days. Then U87 cells (1×10^6) with genetic alterations in 100 μl PBS were subcutaneously injected into both flanks of the mice. Every group contained at least 3 mice. Tumor growth was measured by caliper measurement every 3 days, and tumor volume was calculated after tumor plumped with the formula (volume = tumor length × width2 × π/6). At the termination of the experiment, mice were autopsied and tumors were removed and weighed. All animal experiments were pre-approved and supervised by the Institutional Animal Care and Use Committees of the Southwest University and Experimental Animal Care and Use Committees of the Institute of Sericulture and Systems Biology.

2.15. Data analysis and statistical methodology

All the clinical data were downloaded from the R2: Genomics Analysis and Visualization Platform (https://hgserver1.amc.nl). All the data collected were analyzed by using the Grapgpad Prism 6. Two-tailed unpaired student's *t*-test was applied to determine the significance between different groups. For survival analysis, log-rank (Mantel-Cox) test was conducted. For the correlations of two genes, linear regression analysis in the Grapgpad Prism 6 was used by using 95% confidence interval. For heatmap, the software Heml 1.0 [25] was used to generate images. *P* value < .05 was considered as significant. All the experiments were biologically repeated at least in triple.

3. Results

3.1. FKHRL1/FOXO3a low expression predicts poor prognosis of patients with glioma

To determine the role of FKHRL1 in GBM, we firstly analyzed the relationship between FKHRL1 expression and the prognosis of patients with glioma in a database termed Tumor Glioma Kawaguchi-50-MAS5.0-u133p2 from the R2 platform. The result showed that FKHRL1 expression determined by three different probes was positively correlated with the overall survival (OS) in this cohort (p = 1.3e-4, 1.7e-3 and 6.8e-7, respectively; Fig. 1A, Supplementary Fig. 1A and B). In addition, we analyzed the expression of FKHRL1 in a database termed Tumor Glioblastoma from The Cancer Genome Atlas (TCGA). The results showed that FKHRL1 expression was positively correlated with both OS and progression-free survival (PFS) in this cohort (p = .0055 and .0379, respectively; Fig. 1B and C). Besides, in a database termed Tumor Glioma Lee-100-MAS5.0-u133a from the R2 platform, we found that FKHRL1 expression was lower in WHO grade IV gliomas (p = .0376), compared with that of WHO grade III gliomas, which were less malignant (Fig. 1D). Furthermore, in a database termed Tumor Glioma Sun-153-MAS5.0-u133p2, we found that FKHRL1 expression determined with three different probes was lower in GBM and astrocytroma, compared with that of oligodendrioglioma (Fig. 1E, Supplementary Fig. 1C and D).

In addition, in an experiment termed Exp Glioblastoma (invasion genes) Tofilon-24-MAS5.0-u133a, we found that FKHRL1 expression was lower in GBM cells, compared with that in neural cells (p = .0183; Fig. 1F). Even in GBM spheres with full stem (GSf), the expression of FKHRL1 was lower than that in GBM spheres with restricted stem (GSr) in the experiment termed Exp Glioblastoma Sphere Guenter-17-MAS5.0-u133p2 (p = .0404; Fig. 1G). Actually, FKHRL1 expression was also lower in GBM stem cells than that in neural stem cells experiment in the experiment termed Exp Glioblastoma (invasion genes) Tofilon-24-MAS5.0-u133a (Supplementary Fig. 1E). Besides which, FKHRL1 expression was also lower in recurrent gliomas than that of primary gliomas in the database termed Tumor Glioma Lee-100-MAS5.0-u133a (p = .0292; Fig. 1H).

Since the malignancy of glioma was highly associated with some mutations such as IDH1/2, EGFR, TP53, CIC and H3F3A, we tried to analyze the correlation of FKHRL1 expression with these mutations. IDH1 R132 mutations predicted better survival [26], and we found that FKHRL1 expression was higher in gliomas with IDH1 R132 mutations than wild-type gliomas in the database termed Tumor Glioma French-284-MAS5.0-u133p2 (p = .0003; Fig. 1I). CIC mutation predicted poor outcome of glioma patients [27,28], however, FKHRL1 expression has

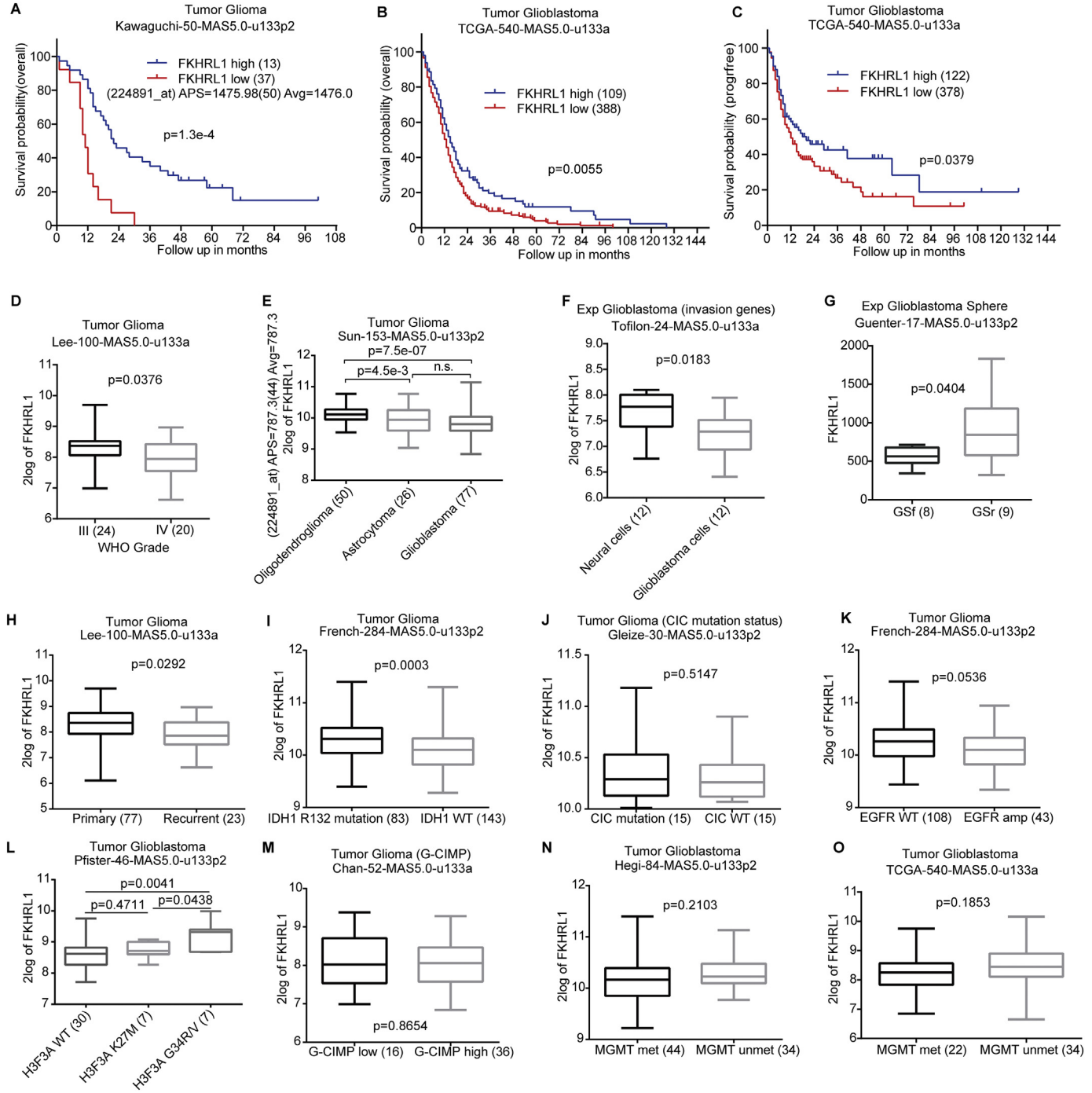

Fig. 1. FKHRL1 low expression predicts poor prognosis of patients with glioma. (A) The relationship between FKHRL1 expression and the overall survival probability in the database termed Tumor Glioma Kawaguchi-50-MAS5.0-u133p2 from the R2 platform. (B and C) The relationship between FKHRL1 expression and the overall survival probability or progression-free survival probability in the database termed Tumor Glioblastoma TCGA-540-MAS5.0-u133a. (D) The expression of FKHRL1 in WHO grade III and IV gliomas in the database termed Tumor Glioma Lee-100-MAS5.0-u133a. (E) The expression of FKHRL1 in different classifications of gliomas including oligodendriaglioma, astrocytoma and glioblastoma in the database termed Tumor Glioma Sun-153-MAS5.0-u133p2. (F) The expression of FKHRL1 in normal neural cells and GBM cells in the database termed Exp Glioblastoma (invasion genes) Tofilon-24-MAS5.0-u133a. (G) The expression of FKHRL1 in glioblastoma spheres with full stem (GSf) and glioblastoma spheres with restricted stem (GSr) in the database termed Exp Glioblastoma Sphere Guenter-17-MAS5.0-u133p2. (H) The expression of FKHRL1 in primary or recurrent glioma in the database termed Tumor Glioma Lee-100-MAS5.0-u133a. (I) The expression of FKHRL1 in gliomas with IDH1 R132 mutation or IDH1 wild type (WT) in the database termed Tumor Glioma French-284-MAS5.0-u133p2. (J) The expression of FKHRL1 in CIC mutant or wild-type gliomas in the database termed Tumor Glioma (CIC mutation status) Gleize-30-MAS5.0-u133p2. (K) The expression of FKHRL1 in gliomas with EGFR amplification or wild-type gliomas in the database termed Tumor Glioma French-284-MAS5.0-u133p2. (L) The expression of FKHRL1 in gliomas with H3F3A mutation or wild-type gliomas in the database termed Tumor Glioblastoma Pfister-46-MAS5.0-u133p2. (M) The expression of FKHRL1 in G-CIMP low or high gilomas in the database termed Tumor Glioma (G-CIMP) Chan-52-MAS5.0-u133a. (N and O) The expression of FKHRL1 in gliomas with MGMT methylation or unmethylation in the databases termed Tumor Glioblastoma Hegi-84-MAS5.0-u133p2 and Tumor Glioblastoma TCGA-540-MAS5.0-u133a.

no correlations with CIC mutation in the database termed Tumor Glioma (CIC mutation status) Gleize-30-MAS5.0-u133p2. (Fig. 1J). EGFR amplification also predicted poor prognosis of glioma [29], however, FKHRL1 expression was also not decreased significantly (p = .0536), compared with that in wild-type gliomas in the database termed Tumor Glioma French-284-MAS5.0-u133p2 (p = .0536; Fig. 1K). Epigenetic marker H3F3A K27M and G34R/V mutations were used as marks for different subgroups of GBMs [30], but in the database termed Tumor Glioblastoma Pfister-46-MAS5.0-u133p2, we found that FKHRL1 expression had no correlations with H3F3A K27M mutations, which predicted a worse prognosis, compared with wild-type groups (Fig. 1L). However, FKHRL1 expression was higher in H3F3A G34R/V mutant groups, which had a better prognosis, compared with wild-type or K27M mutant groups (p = .0041 and 0.0438, respectively; Fig. 1L). G-CIMP low group usually had a poorer clinical outcome in recurrent glioma than G-CIMP high group [31], however, we found no correlations of FKHRL1 expression between G-CIMP high group and G-CIMP low group, in the database termed Tumor Glioma (G-CIMP) Chan-52-MAS5.0-u133a (Fig. 1M). MGMT methylation often predicted better prognosis of gliomas during temozolomide treatment [32], however, we found that FKHRL1 also had no correlations with MGMT methylation status in the databases termed Tumor Glioblastoma Hegi-84-MAS5.0-u133p2 and Tumor Glioblastoma TCGA-540-MAS5.0-u133a (Fig. 1N and O). These results showed that FKHRL1 expression was correlated with IDH1 R132 mutation and H3F3A G34R/V mutations.

All these evidences showed that FKHRL1 expression was positively related with the prognosis of patients with gliomas, and its low expression in gliomas and GBM stem cells and high expression in IDH1 R132 mutant or H3F3A G34R/V mutant gliomas implied that FKHRL1 might be an important suppressor in glioma.

3.2. FKHRL1/FOXO3a silencing promotes the Warburg effect and cell proliferation of HEB gliocytes

As FKHRL1 might be a tumor suppressor in glioma, we silenced its expression in HEB gliocytes by using stable lenti-viruses-mediated knockdown (Fig. 2A). Then we detected glucose uptake by using 2-NBDG and flow cytometry. FKHRL1 silencing significantly promoted glucose uptake of HEB cells (Fig. 2B). GO assay was used to detect glucose consumption and the result showed that FKHRL1 silencing remarkably upregulated glucose consumption, too (Fig. 2C). Besides this, lactate production and LDH activities were also increased significantly in FKHRL1-silenced HEB cells, compared with control groups (Fig. 2D and E). Importantly, FKHRL1 silencing also promoted cell proliferation and growth of HEB cells (Fig. 2F–H). These results implied that FKHRL1 is negatively correlated with cell proliferation and glycolysis.

3.3. FKHRL1/FOXO3a expression is tightly correlated with SIRT6 and glycolytic genes expression in gliomas

Since the Warburg effect was important for tumor progression, we explored whether FKHRL1 also contributed to cell metabolism in GBM. SIRT6 was reported as a major regulator of glycolysis [33]. Surprisingly, we found that FKHRL1 expression was positively correlated with the SIRT6 expression in several different databases including Tumor Glioma French-284-MAS5.0-u133p2 (r-value = .329, p-value = 1.3e-08), Tumor Glioma Kawaguchi-50-MAS5.0-u133p2 (r-value = .315, p-value = .03), Tumor Glioma Sun-153-MAS5.0-u133p2 (r-value = .212, p-value = 8.6e-03; r-value = .201, p-value = .01), Tumor Glioma (G-CIMP) Chan-52-MAS5.0-u133a (r-value = .329, p-value = .02) and Tumor Glioblastoma TCGA-395-MAS5.0-u133a (r-value = .111, p-value = .03) from the R2 platform (Fig. 3A–E and Supplementary Fig. 2A). In addition, the expression of FKHRL1 was negatively correlated with the expression of several important glycolytic genes including GLUT1 (r-value = .167, p-value = 4.8e-3), GLUT4 (r-value = .146, p-value = .01), HK1 (r-value = .201, p-value = 6.6e-4), HK2 (r-value = .367, p-value = 1.7e-10), HK3 (r-value = .343, p-value = 2.9e-9), GAPDH (r-value = .286, p-value = 3.4e-4), PFKFB3 (r-value = .233, p-value = 7.3e-5), PKM (r-value = .203, p-value = 2.1e-6) and LDHA (r-value = .213, p-value = 6.2e-7) in several glioma cohorts (only r-value and p-value of main figures were shown; Fig. 3F–N and Supplementary Fig. 2B–X). Importantly, we clustered FKHRL1 expression with the expression of SIRT6 and some glycolytic genes in the database termed Tumor Glioma French-284-MAS5.0-u133p2 and generated a heatmap by using Heml 1.0, the result in Fig. 3O showed that FKHRL1 expression was positive correlated with SIRT6 expression, while it was negatively correlated with the expression of a cluster of glycolytic genes, such as SLC2A1 (GLUT1), SLC2A4 (GLUT4), HK1, HK2, GAPDH, PFKFB3, LDHA, GPI, PGK1, ADPGK, ENO1, SLC16A1 (MCT1) and SLC16A4 (MCT4). These results indicated that FKHRL1 expression was positively correlated with SIRT6 expression and negatively correlated with glycolytic genes expression in glioma.

3.4. SIRT6 overexpression impairs aerobic glycolysis promoted by FKHRL1/FOXO3a silencing

Based on the results above, we explored the relationship between FKHRL1 and SIRT6 in established GBM cells. FKHRL1 was knockdown in U251 GBM cells through lenti-virus transduction. Then qRT-PCR and Western blot was performed to detect the infection efficiency. The results showed that SIRT6 expression was downregulated after FKHRL1 silencing (Fig. 4A and B). Afterwards, we restored SIRT6 in the FKHRL1-silenced cells (Fig. 4I and C). Then we analyzed glucose uptake by virtue of flow cytometry with the help of a fluorescigenic glucose analogue 2-NBDG. The result showed that FKHRL1 silencing promoted glucose uptake in U251 cells, while SIRT6 restoration recovered the effect of FKHRL1 silencing (Fig. 4D). Furthermore, we confirmed this result by using a GO assay kit to detect the glucose content in the medium after cells culture for 48 h, and then glucose consumption was calculated. The result showed that FKHRL1 silencing promoted glucose consumption, which was also recovered by SIRT6 overexpression (Fig. 4E). Similarly, Lactate production and LDH activities were also promoted by FKHRL1 silencing, and SIRT6 overexpression rescued the effect of FKHRL1 silencing (Fig. 4F and G). Then the glycolytic stress flux test was conducted on the Seahorse XF analyzer to assess changes in glycolytic flux resulting from FKHRL1 silencing and SIRT6 restoration. The result showed that glycolytic flux was increased after FKHRL1 knockdown and was retrieved again *via* SIRT6 restoration (Fig. 4H). Then we checked the expression of several known glycolytic genes, including *glut4, glut1, hk1, hk2, hk3, gapdh, pfk1, pkm2, idh-a1* and *idh-a2*, that were targeted by SIRT6, and found all of them were significantly upregulated, while SIRT6 re-overexpression recovered the result induced by FKHRL1 silencing (Fig. 4I). These results showed that FKHRL1 might function as an upstream factor of SIRT6, thereby affecting aerobic glycolysis in GBM cells.

3.5. SIRT6 silencing rescues downregulated aerobic glycolysis induced by FKHRL1/FOXO3a overexpression

To further confirm our results, we overexpressed FKHRL1 in U251 cells, and the result showed that SIRT6 was upregulated after FKHRL1 overexpression (Fig. 5A and B). As expected, FKHRL1 overexpression inhibited glucose uptake, glucose consumption, lactate production, LDH activity, glycolytic flux and the expression of SIRT6-targeted glycolytic genes (Fig. 5C–I). Moreover, SIRT6 silencing also rescued FKHRL1 overexpression-induced decline of glycolysis (Fig. 5C–I). Collectively, these results further confirmed that SIRT6 functioned as a downstream factor of FKHRL1 in the regulation of the Warburg effect.

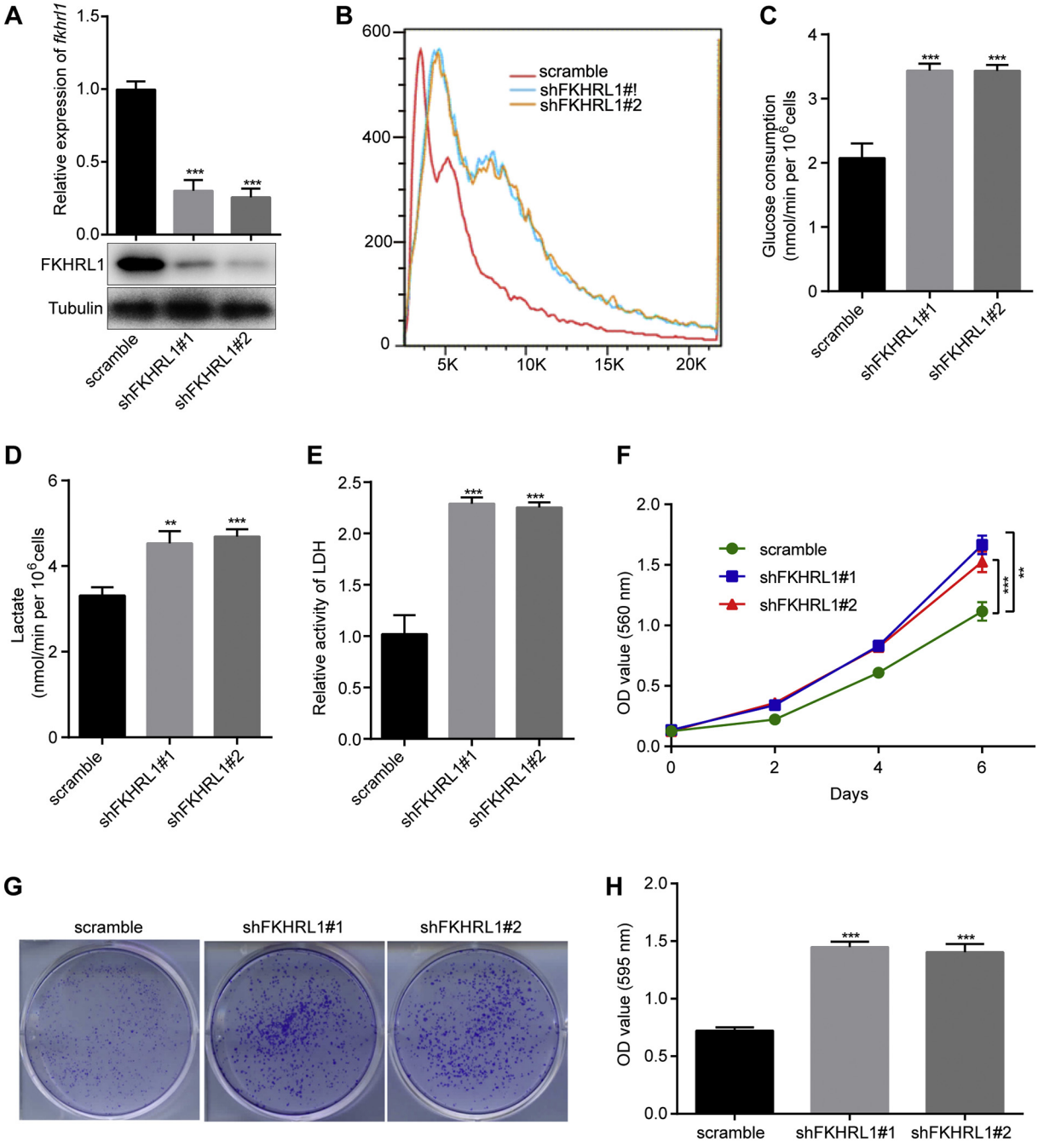

Fig. 2. FKHRL1 silencing promotes aerobic glycolysis in normal gliocytes. (A) The relative expression of FKHRL1 was detected by qRT-PCR and protein expression level of FKHRL1 was detected by Western blot in FKHRL1-silenced HEB cells. (B) Glucose uptake was detected by flow cytometery in the 2-NBDG treated FKHRL1-silenced HEB cells. (C) Glucose consumption was detected by using a GO assay kit in the 2-NBDG-treated FKHRL1-silenced HEB cells. (D) Lactate production was detected by using a lactate assay kit in FKHRL1-silenced HEB cells. (E) The lactate dehydrogenase activities were detected by using a lactate dehydrogenase assay kit in FKHRL1-silenced HEB cells. (F) Growth curve was determined by the MTT assay in FKHRL1-silenced HEB cells. (G and H) Cell viabilities were determined by flat plate clone formation test in FKHRL1-silenced HEB cells. *$p < .05$, **$p < .01$, ***$p < .001$, n.s., non-sense.

3.6. *FKHRL1/FOXO3a transcriptionally promotes the expression of SIRT6*

To elucidate the molecular mechanism of FKHRL1 in regulation of SIRT6 expression, we next tried to explore whether SIRT6 expression could be transcriptionally regulated by FKHRL1. Previous reports had shown that FKHRL1 could regulate the expression of SIRT6 by binding and activating transcriptional factor NRF1 in the mouse [34]. However, we didn't find any NRF1 binding sites (AGGGCGCATGCGCCCTC) in the promoter regions (−2500 to 0) of human SIRT6. This implied that FKHRL1 might have another mechanism to regulate the transcription of SIRT6. Then we aligned −2500 to 0 bp in the promoter region of mouse SIRT6 and human SIRT6 by using the online Bl2seq tool in the SilkDB (http://www.silkdb.org/silkdb/). The results showed that there are several DNA fragments with the same sequence in both promoters (Fig. 6A). We hypothesized that some of these fragments might be important for recognizing and binding for FKHRL1 in the promotor of SIRT6. Later, we cloned several regions (which were termed 0.1 k, 0.2 k, 0.6 k, 1.2 k and −0.9 k) from the promoter of human SIRT6 and constructed them into the pGL3 vector. The result of dual luciferase assay showed that only 1.2 k regions displayed a significant high

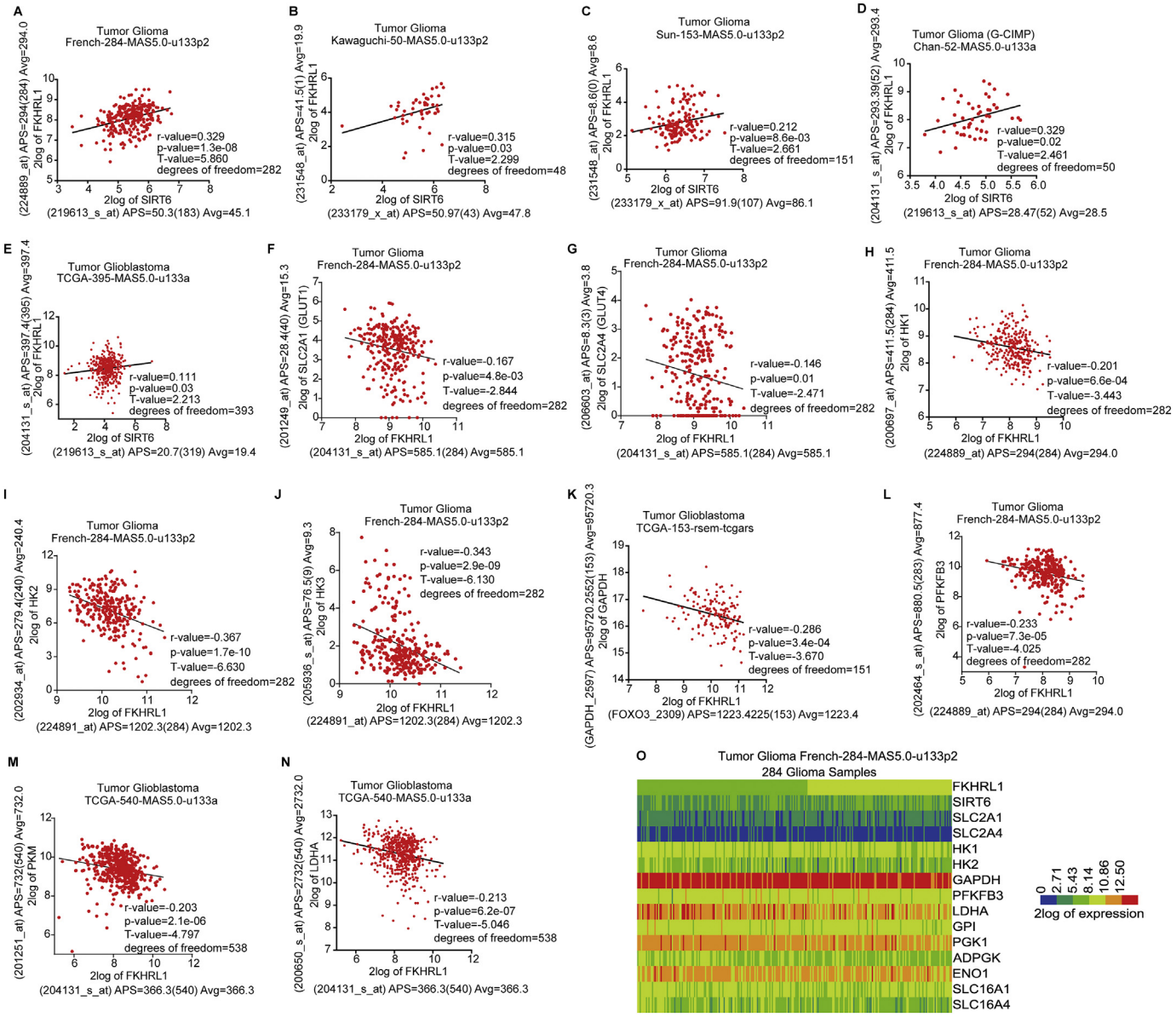

Fig. 3. FKHRL1 expression is positively correlated with SIRT6 expression. (A to E) The correlation of FKHRL1 expression and SIRT6 expression in 5 different glioma or GBM cohorts. (F to N) The correlation of FKHRL1 expression and expression of SIRT6 target genes including SLC2A1 (GLUT1), SLC2A4 (GLUT4), HK1, HK2, HK3, GAPDH,PFKFB3, PKM and LDHA in several glioma cohorts. (O) The heatmap of the expression of FKHRL1, SIRT6 and a cluster of glycolytic genes in gliomas in the database termed Tumor Glioma French-284-MAS5.0-u133p2.

activity, compared with other regions (Fig. 6B). Besides, FKHRL1 knockdown also impaired the activity of 1.2 k regions in U251 cells (Fig. 6C). These results implied that there was a binding site for FKHRL1 in the −2128∼−1514 bp region of SIRT6 promoter. Since there were four candidate FKHRL1 binding sites in this region, we used the ChIP qRT-PCR to detect the exact binding site. The results revealed that FKHRL1 has a significant enrichment in the regions containing the first two candidate binding sites (−2083 to −1859 bp), while has no enrichment in regions containing the last two candidate binding sites (−1852 to −1746, Fig. 6D and E). Later, we downloaded the logo of human FKHRL1 binding profile from the JASPER (http://jaspar.binf.ku.dk/; Fig. 6F). From the first two candidate binding sites (−2083 to −1859 bp, the product of Primer1) we found a site that was highly similar with human FKHRL1 binding profile (Fig. 6G). Then we synthesized a mutant Primer1 product and constructed into pGL3 vector. Luciferase result indicated that mutant Primer1 product lost promoter activity, compared with wild-type Primer1 product or the 1.2 k region (Fig. 6H). These results indicated that FKHRL1 regulated SIRT6 expression *via* a transcriptional manner that is different from the regulatory mode identified in the mouse.

3.7. FKHRL1/FOXO3a - SIRT6 axis regulates GBM growth in vitro and in vivo

To elucidate FKHRL1-SIRT6 axis in the development of GBM, we subsequently analyzed its function on cell growth of GBM cells *in vitro* and *in vivo*. We constructed FKHRL1-silenced U251 and U87 cells and then recovered by FKHRL1 or SIRT6 using lenti-virus-mediated stable transfection (7A). MTT assay showed that cell proliferation was promoted in U251 and U87 cells after FKHRL1 knockdown, and the effect of FKHRL1 knockdown was recovered by FKHRL1 restoration or SIRT6 overexpression (Fig. 7B and C).

Later, we confirmed the cell growth of GBM in the xenograft models. We subcutaneously injected 1×10^6 U87 GBM cells with

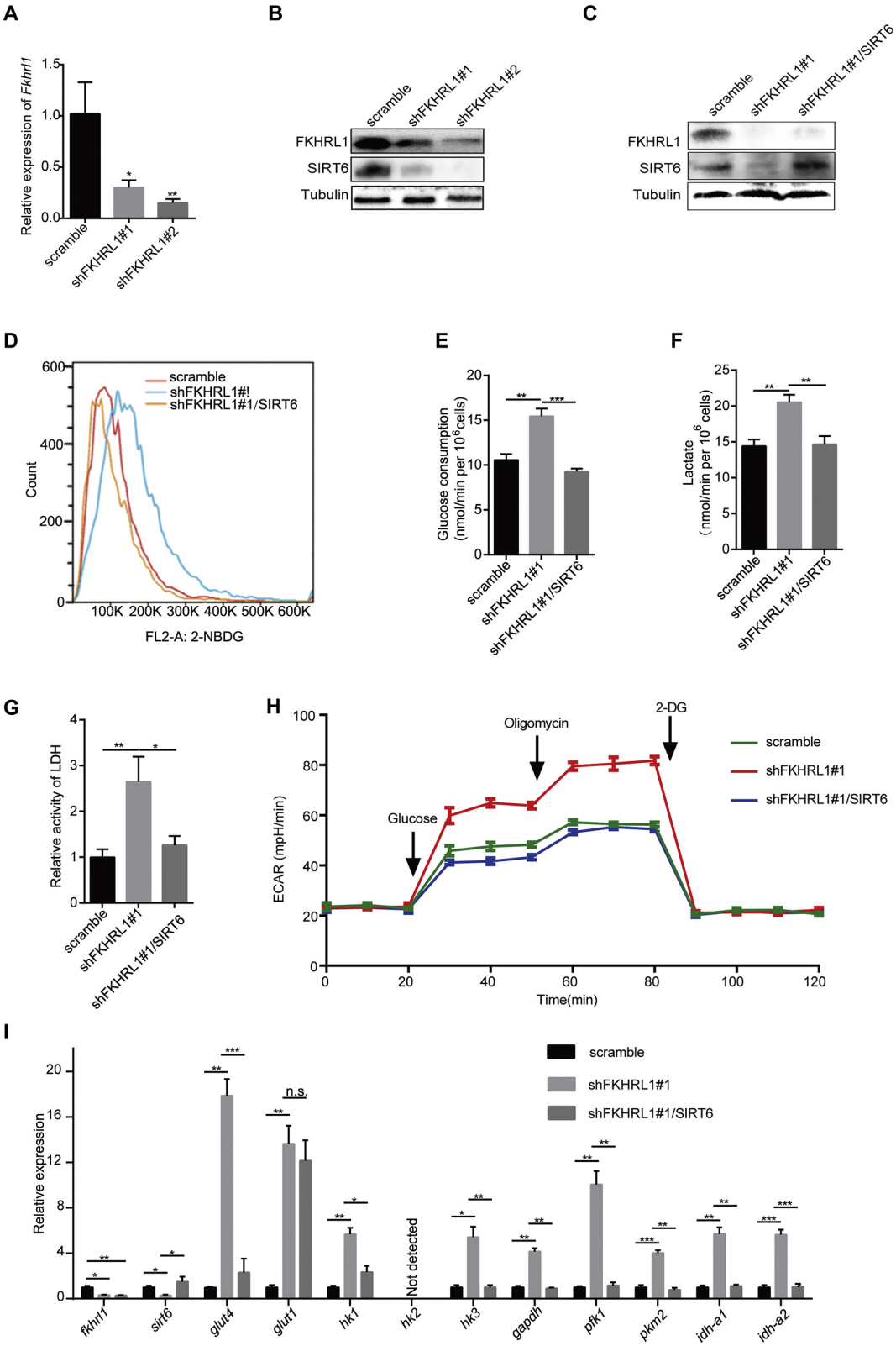

Fig. 4. SIRT6 overexpression impairs aerobic glycolysis promoted by FKHRL1 silencing. (A) The relative expression of FKHRL1 was detected by qRT-PCR in U251 GBM cells after FKHRL1 silencing. (B) The expression of FKHRL1 and SIRT6 were detected by Western blot in U251 GBM cells after FKHRL1 silencing. (C) The expression of FKHRL1 and SIRT6 were detected by Western blot in FKHRL1-silenced U251 GBM cells after SIRT6 restoration. (D) Glucose uptake was detected by flow cytometery in the 2-NBDG-treated FKHRL1-silenced U251 GBM cells after SIRT6 restoration. (E) Glucose consumption was detected by using a GO assay kit in the 2-NBDG-treated FKHRL1-silenced U251 GBM cells after SIRT6 restoration. (F) Lactate production was detected by using a lactate assay kit in FKHRL1-silenced U251 GBM cells after SIRT6 restoration. (G) The lactate dehydrogenase activities were detected by using a lactate dehydrogenase assay kit in FKHRL1-silenced U251 GBM cells after SIRT6 restoration. (H) The glycolytic stress flux test was conducted on the Seahorse XF analyzer to assess changes in glycolytic flux resulting from FKHRL1 silencing and SIRT6 restoration. ECAR, extracellular acidification rate. (I) The relative expression of SIRT6 target glycolytic genes were detected by qRT-PCR in FKHRL1-silenced U251 GBM cells after SIRT6 restoration. $*p < .05$, $**p < .01$, $***p < .001$, n.s., non-sense.

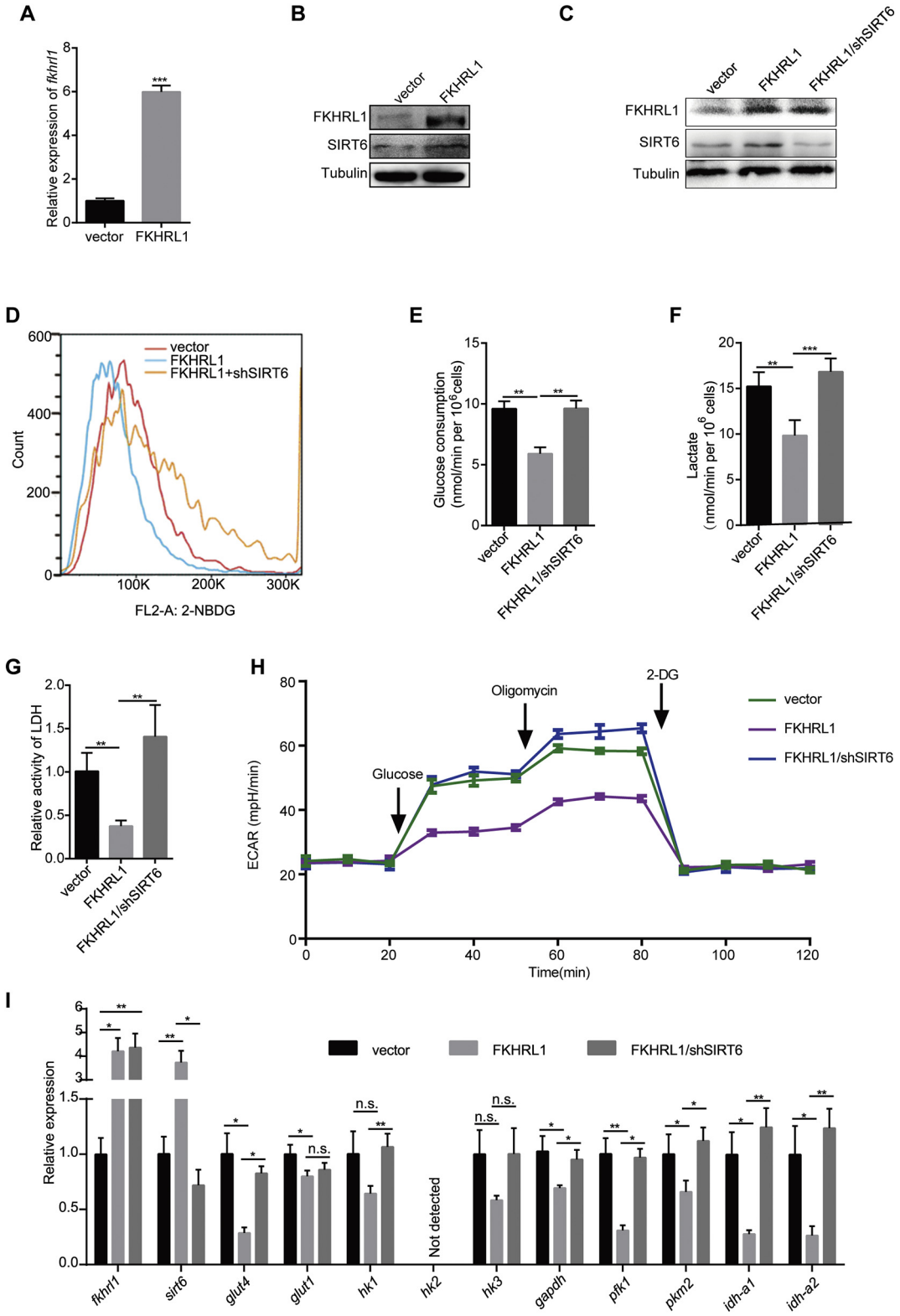

Fig. 5. SIRT6 silencing rescues downregulated aerobic glycolysis induced by FKHRL1 overexpression. (A) The relative expression of FKHRL1 was detected by qRT-PCR in U251 GBM cells after FKHRL1 overexpression. (B) The expression of FKHRL1 and SIRT6 were detected by Western blot in U251 GBM cells after FKHRL1 overexpression. (C) The expression of FKHRL1 and SIRT6 were detected by Western blot in FKHRL1-overexpressed U251 GBM cells after SIRT6 silencing. (D) Glucose uptake was detected by flow cytometery in the 2-NBDG-treated FKHRL1-overexpressed U251 GBM cells after SIRT6 silencing. (E) Glucose consumption was detected by using a GO assay kit in the 2-NBDG-treated FKHRL1-overexpressed U251 GBM cells after SIRT6 silencing. (F) Lactate production was detected by using a lactate assay kit in FKHRL1-overexpressed U251 GBM cells after SIRT6 silencing. (G) The lactate dehydrogenase activities were detected by using a lactate dehydrogenase assay kit in FKHRL1-overexpressed U251 GBM cells after SIRT6 silencing. (H) The glycolytic stress flux test was conducted on the Seahorse XF analyzer to assess changes in glycolytic flux resulting from FKHRL1 overexpression and SIRT6 knockdown. ECAR, extracellular acidification rate. (I) The relative expression of SIRT6 target glycolytic genes were detected by qRT-PCR in overexpressed-U251 GBM cells after SIRT6 silence. *p < .05, **p < .01, ***p < .001, n.s., non-sense.

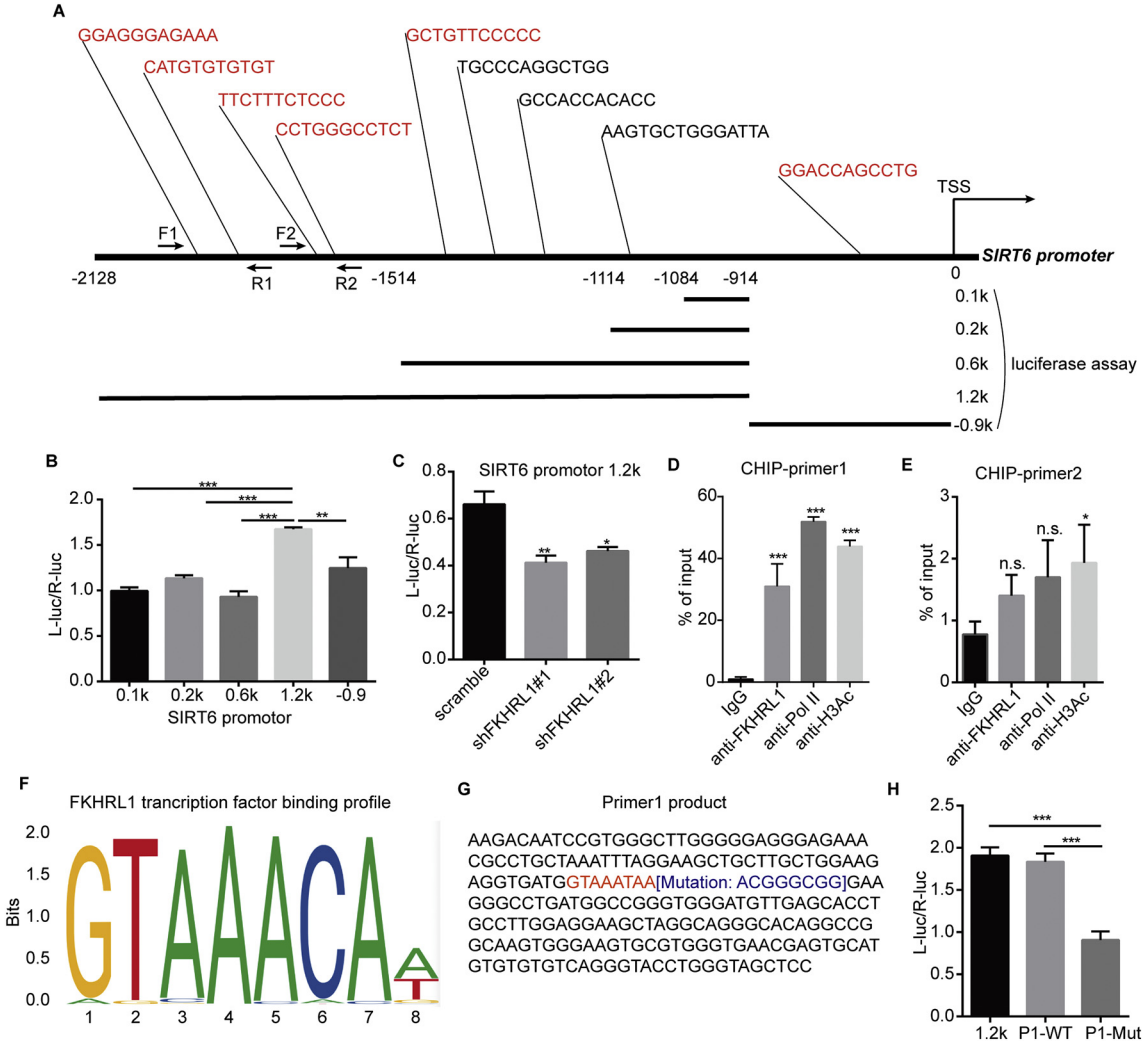

Fig. 6. FKHRL1 transcriptionally promotes the expression of SIRT6. (A) Overview of designed CHIP primers and insert fragments in pGL3 vectors used in the dual luciferase assay in the promoter of human SIRT6 genes. (B) SIRT6 promoter (with different regions) activities were detected by the dual luciferase assay in 293FT cells. F-luc/R-luc, Firefly luciferase/Renilla luciferase. (C) SIRT6 promoter activities detected by the dual luciferase assay in U251 cells after FKHRL1 silencing. (D and E) CHIP qRT-PCR assay was performed to detect the enrichment of FKHRL1 in the promoter region of SIRT6 in U251 cells. Ant-Pol II and anti-H3Ac antibodies were used as positive controls, while IgG was used as a negative control. (F) Logo of human FKHRL1 transcription factor binding profile downloaded from the JASPAR development server (http://jaspar.binf.ku.dk/). (G) The products of Primer1. The nucleotides similar to FKHRL1 transcription factor binding profile is marked red. The mutation information is shown blue. (H) SIRT6 promoter with 1.2 k region, wild-type Primer1 product (P1-WT) and mutant Primer1 product (P1-Mut) activities were detected by the dual luciferase assay in 293FT cells. *p < .05, **p < .01, ***p < .001, n.s., non-sense. (For interpretation of the references to colour in this figure legend, the reader is referred to the web version of this article.)

indicated infection, and calculated volumes of the pumped tumors every 5 days. The results showed that FKHRL1 silencing significantly promoted cell growth *in vivo* and the effect was rescued by both FKHRL1 and SIRT6 overexpression (Fig. 7D and E). After 35 days, mouse were autopsied and tumors were taken out and weighed, the result showed that FKHRL1 silencing significantly increased the weight of tumors, while FKHRL1 and SIRT6 overexpression recovered the effect of FKHRL1 silencing (Fig. 7F). Besides, we also showed that tumors formed from FKHRL1-silenced U87 cells uptook more glucose, produced more lactate and upregulated a cluster of glycolytic genes than scramble groups, while FKHRL1 or SIRT6 overexpression retrieved the effect of FKHRL1 silencing (Fig. 7G–I). These results showed that FKHRL1-SIRT6 axis played an essential role in cell metabolism and development of GBM cells *in vivo*.

4. Discussion

Metabolic reprogramming was important malignant adaption for GBM. Glucose metabolic alterations including metabolic flux involving mitochondrial dynamics and the Warburg effect were essential for cell growth, metastasis and stemness of GBM cells. Inhibition of glucose metabolism in GBM might be a promising efficient method to treat GBM. For instance, a synthetic small-molecule KHS101 could impair both mitochondrial bioenergetic capacity and glycolytic activity to inhibit GBM growth in mice [35]. Coordinated upregulation of autophagy followed by its inhibition could disrupt mitochondrial bioenergetics to make GBM cells sensitive to chemotherapy [36]. In addition to mitochondrial energy modulation, reversing the Warburg effect might be another promising strategy for GBM treatment [37]. Combination treatment with 2-deoxyglucose, a glycolysis inhibitor, and metformin could inhibit GBM tumorspheres [38]. Treatment with dichloroacetate, a PDK inhibitor, also sensitized GBM cells to irradiation [39]. Silencing of a glycolytic LDHA gene sensitized GBM cells to radiation and temozolomide [40]. NAMPT inhibition induced glycolysis down-regulation was selectively toxic for MYC or MYCN-amplified GBM [11]. Besides, glycolytic enzyme localization was also an important reason

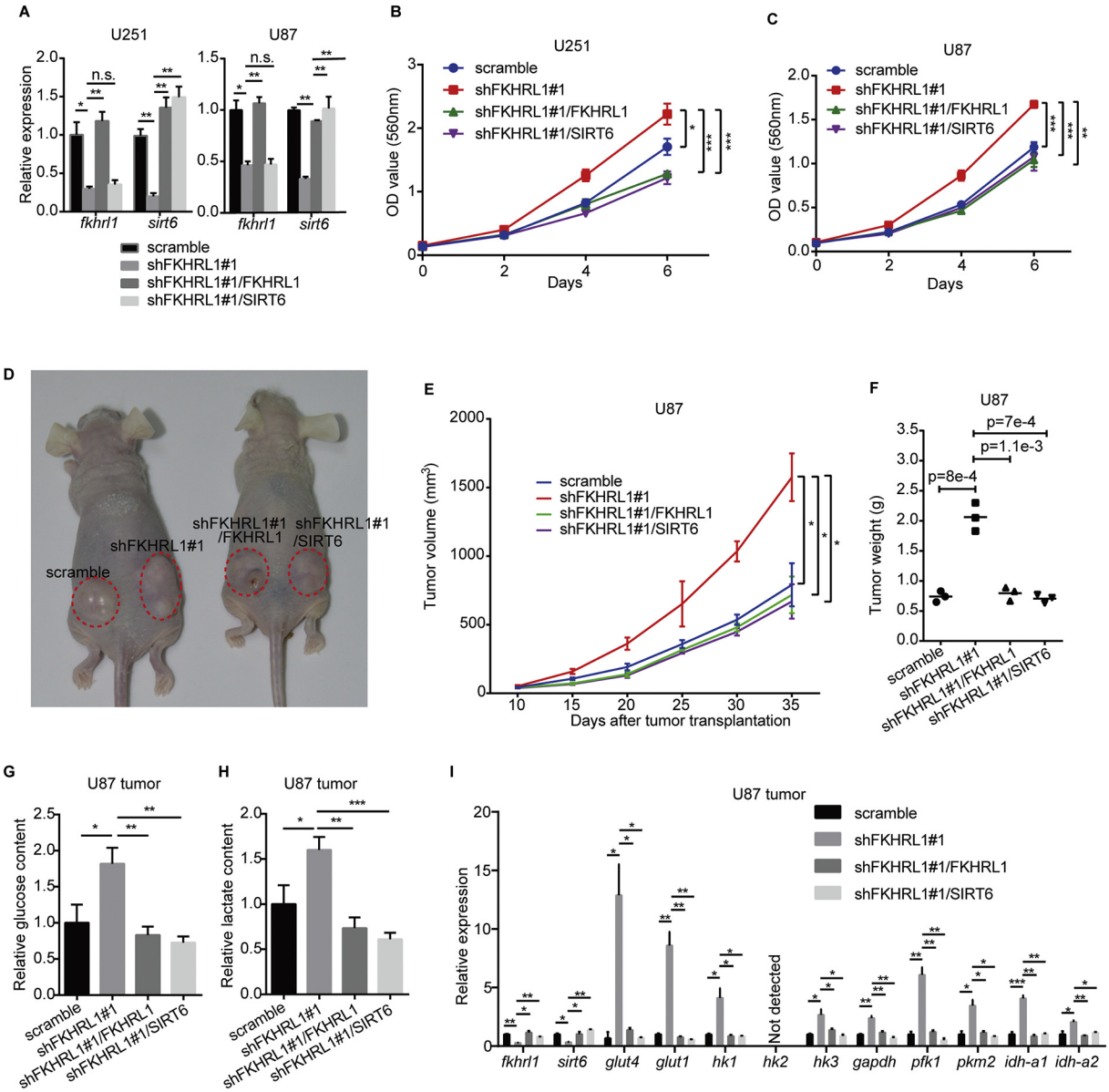

Fig. 7. FKHRL1-SIRT6 axis regulates GBM growth *in vitro* and *in vivo*. (A) The relative expression of FKHRL1 and SIRT6 were detected by qRT-PCR in FKHRL1/scramble silenced-U251/U87 GBM cells after FKHRL1 or SIRT6 overexpression. (B and C) Growth curve was determined by the MTT assay in FKHRL1/scramble silenced-U251/U87 GBM cells after FKHRL1 or SIRT6 overexpression. (D) The tumor growth for 5 weeks of in FKHRL1/scramble silenced-U87 GBM cells after FKHRL1 or SIRT6 overexpression in the BALB/c-nu mice. (E) The volume of tumors formed from FKHRL1/scramble silenced-U87 GBM cells after FKHRL1 or SIRT6 overexpression in the BALB/c-nu mice was calculated. (F) The weight of tumors formed from FKHRL1/scramble silenced-U87 GBM cells after FKHRL1 or SIRT6 overexpression in the BALB/c-nu mice. (G) Relative glucose content (normalized by protein weight) in tumors formed from FKHRL1/scramble silenced-U87 GBM cells after FKHRL1 or SIRT6 overexpression in the BALB/c-nu mice. (H) Relative lactate content (normalized by protein weight) in tumors formed from FKHRL1/scramble silenced-U87 GBM cells after FKHRL1 or SIRT6 overexpression in the BALB/c-nu mice. (I) Relative expression of SIRT6 target glycolytic genes in tumors formed from FKHRL1/scramble silenced-U87 GBM cells after FKHRL1 or SIRT6 overexpression in the BALB/c-nu mice. *p < .05, **p < .01, ***p < .001, n.s., non-sense.

for tumor malignancy and these enzymes could be considered as therapeutic targets, too. For example, hexokinase II could translocate into mitochondria to suppress cell death of cancer cells, and 3-bromopyruvate was shown as a promising molecule to target it [41,42]. These evidences indicated that glycolysis was important for GBM progression and inhibiting glycolysis might be a novel strategy for GBM treatment. However, the molecular mechanism of the Warburg effect had not been fully elucidated.

SIRT6 had been shown to be a major regulator in cell metabolism, especially in glycolysis [33]. SIRT6 could directly deacetylate histone 3 lysine 9 (H3K9) to control the expression of a cluster of glycolytic genes, including *glut1, pdk4, pdk1, aldoc, pfk1, ldhb, ldha, tpi5* and *gapdh*; meanwhile, SIRT6 also functioned as a corepressor of the transcriptional factor Hif1α and c-Myc, critical regulators of glycolysis [33,43]. The crucial function of SIRT6 in the regulation of glycolysis had been also confirmed in various types of tumors, including breast cancer [44], urothelial carcinoma [45] and hepatocellular carcinoma [46].

However, FKHRL1 also showed to regulate the Warburg effect. For example, FKHRL1 binds to and transactivates the TSC1 promoter, thus inhibits glycolysis [47]. FKHRL1 promotes metabolic adaptation to hypoxia by antagonizing Myc function [48]. Surprisingly, clinical data analysis revealed that FKHRL1 expression was positively correlated with SIRT6 expression in several different cohorts. Subsequently, we

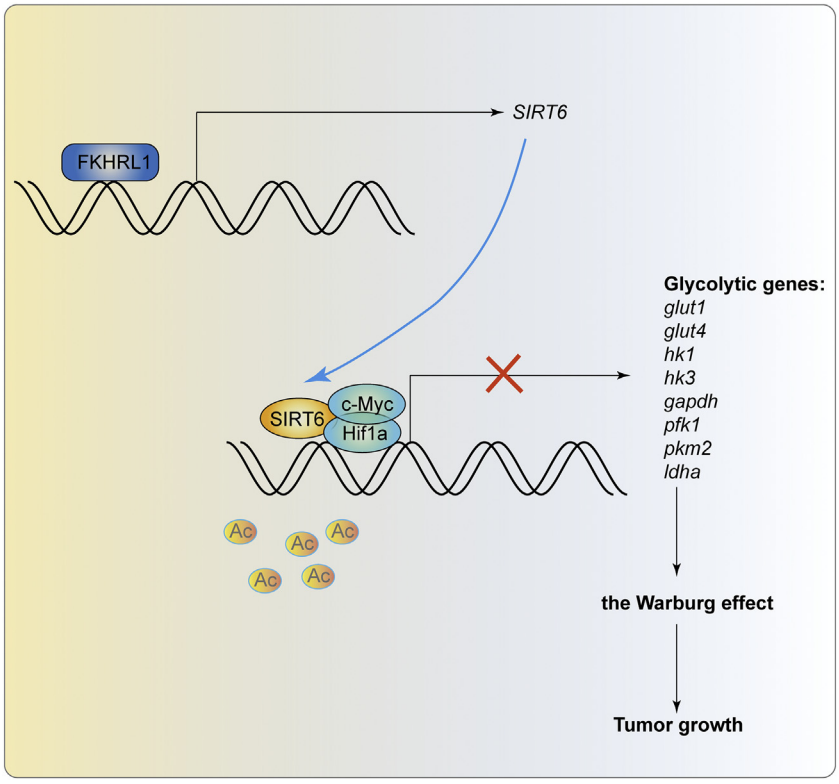

Fig. 8. Model of action of FKHRL1-SIRT6 axis in the regulation of the Warburg effect in glioblastoma cells. FKHRL1 transcriptionally activates SIRT6 expression, which further binds to c-Myc or Hif1a to inhibit the expression of a cluster of glycolytic genes, thereby suppressing the Warburg effect and tumor growth.

confirmed that SIRT6 expression was transcriptionally controlled by FKHRL1. In addition, FKHRL1-controlled glycolysis was also dependent on the expression of SIRT6. Mechanically, FKHRL1 bound to the specific regions of SIRT6 promoter and activated its transcriptional activity. Previous reports had shown that FKHRL1 could regulate the expression of SIRT6 by binding and activating transcriptional factor NRF1 in the mouse [34]. However, there was neither NRF2 binding site (AGGGCGCATGCGCCCTC) nor FKHRL1 binding sites [GTAAACA(A/T)] provided by the JASPER (http://jaspar.binf.ku.dk/) in the promoter region of human SIRT6 promoter. But we found a site (GTAAATAA) in SIRT6 promoter that is highly similar with FKHRL1 binding site [GTA AACA(A/T)] downloaded from the JASPER. Then we made sure that this site was essential for its promoter activity. Our results provided a novel mechanism that FKHRL1 transcriptionally promote SIRT6 expression in GBM.

Indeed, SIRT6-controlled glycolysis had never been explored in GBM. Actually, there were evidences showed that SIRT6 was shown to block glioma growth through promoting apoptosis, inducing oxidative stress resistance [49], inhibiting JAK2/STAT3 signaling pathway [50], suppressing RNA-binding protein PCBP2 [51] and downregulating NOTCH3 signaling [52]. However, the relationship between SIRT6-induced glycolysis and glioma growth had never been confirmed. Herein, we found FKHRL1 knockdown promotes cell proliferation and glycolysis in HEB gliocytes. SIRT6 overexpression could retrieve the promoted glycolysis induced by FKHRL1 silencing in GBM cells. SIRT6 silencing also recovered FKHRL1 overexpression-induced decline of glycolysis in GBM cells. Besides, SIRT6 also retrieved FKHRL1 silencing-induced GBM cell growth. These results showed that FKHRL1-SIRT6 axis played an essential role in the regulation of cell metabolism in GBM.

Collectively, our data showed that FKHRL1 low expression was a promising prognostic marker in GBM. Besides, its expression was significantly correlated with WHO grade of glioma. FKHRL1 inhibited glucose uptake and consumption, thus blocked GBM growth. Mechanically, FKHRL1 promoted SIRT6 transcription, so that to inhibit the expression of a cluster of glycolytic genes (Fig. 8). Our result elucidated a regulatory model of FKHRL1-SIRT6 axis in glycolysis of human GBM, which might provide clues for GBM treatment.

Supplementary data to this article can be found online at https://doi.org/10.1016/j.cellsig.2019.04.009.

Conflict and interest

The authors declare no conflict of interest.

Acknowledgement

We thank Muhammad Nadeem Abbas and Saima Kausar for checking the grammatical arrangement and syntax in the text. We are grateful for funding support from the Project Funded by Chongqing Special Postdoctoral Science Foundation (No. XmT2018080), the Fundamental Research Funds for the Central Universities (XDJK2019C013), the National Key Research and Development Program of China (No. 2016YFC1302204 and 2017YFC1308600) and the National Natural Science Foundation of China (No. 81672502).

References

[1] Q.T. Ostrom, H. Gittleman, P. Farah, A. Ondracek, Y. Chen, Y. Wolinsky, N.E. Stroup, C. Kruchko, J.S. Barnholtz-Sloan, CBTRUS statistical report: primary brain and central nervous system tumors diagnosed in the United States in 2006–2010, Neuro-oncology 15 (Suppl. 2) (2013) (ii1-56).
[2] R. Stupp, W.P. Mason, M.J. van den Bent, M. Weller, B. Fisher, M.J. Taphoorn, K. Belanger, A.A. Brandes, C. Marosi, U. Bogdahn, J. Curschmann, R.C. Janzer, S.K. Ludwin, T. Gorlia, A. Allgeier, D. Lacombe, J.G. Cairncross, E. Eisenhauer, R.O. Mirimanoff, Radiotherapy plus concomitant and adjuvant temozolomide for glioblastoma, N. Engl. J. Med. 352 (10) (2005) 987–996.
[3] K. Messaoudi, A. Clavreul, F. Lagarce, Toward an effective strategy in glioblastoma treatment. Part I: resistance mechanisms and strategies to overcome resistance of glioblastoma to temozolomide, Drug Discov. Today 20 (7) (2015) 899–905.
[4] D. Hanahan, R.A. Weinberg, Hallmarks of cancer: the next generation, Cell 144 (5)

(2011) 646–674.
[5] J.R. Cantor, D.M. Sabatini, Cancer cell metabolism: one hallmark, many faces, Cancer Discov. 2 (10) (2012) 881–898.
[6] M.G. Vander Heiden, L.C. Cantley, C.B. Thompson, Understanding the Warburg effect: the metabolic requirements of cell proliferation, Science (New York, N.Y.) 324 (5930) (2009) 1029–1033.
[7] R. Courtnay, D.C. Ngo, N. Malik, K. Ververis, S.M. Tortorella, T.C. Karagiannis, Cancer metabolism and the Warburg effect: the role of HIF-1 and PI3K, Mol. Biol. Rep. 42 (4) (2015) 841–851.
[8] Z. Dong, H. Cui, Epigenetic modulation of metabolism in glioblastoma, Semin. Cancer Biol. (2018), https://doi.org/10.1016/j.semcancer.2018.09.002.
[9] S. Zhu, Z. Dong, X. Ke, J. Hou, E. Zhao, K. Zhang, F. Wang, L. Yang, Z. Xiang, H. Cui, The roles of sirtuins family in cell metabolism during tumor development, Semin. Cancer Biol. (2018), https://doi.org/10.1016/j.semcancer.2018.11.003.
[10] S. Zhao, H. Liu, Y. Liu, J. Wu, C. Wang, X. Hou, X. Chen, G. Yang, L. Zhao, H. Che, Y. Bi, H. Wang, F. Peng, J. Ai, miR-143 inhibits glycolysis and depletes stemness of glioblastoma stem-like cells, Cancer Lett. 333 (2) (2013) 253–260.
[11] K. Tateishi, A.J. Iafrate, Q. Ho, W.T. Curry, T.T. Batchelor, K.T. Flaherty, M.L. Onozato, N. Lelic, S. Sundaram, D.P. Cahill, A.S. Chi, H. Wakimoto, Myc-driven glycolysis is a therapeutic target in glioblastoma, Clin. Cancer Res. 22 (17) (2016) 4452–4465.
[12] N. Komatsu, T. Watanabe, M. Uchida, M. Mori, K. Kirito, S. Kikuchi, Q. Liu, T. Tauchi, K. Miyazawa, H. Endo, T. Nagai, K. Ozawa, A member of Forkhead transcription factor FKHRL1 is a downstream effector of STI571-induced cell cycle arrest in BCR-ABL-expressing cells, J. Biol. Chem. 278 (8) (2003) 6411–6419.
[13] H. You, Y. Jang, A.I. You-Ten, H. Okada, J. Liepa, A. Wakeham, K. Zaugg, T.W. Mak, p53-dependent inhibition of FKHRL1 in response to DNA damage through protein kinase SGK1, Proc. Natl. Acad. Sci. U. S. A. 101 (39) (2004) 14057–14062.
[14] Z. Radisavljevic, Nitric oxide suppression triggers apoptosis through the FKHRL1 (FOXO3A)/ROCK kinase pathway in human breast carcinoma cells, Cancer 97 (5) (2003) 1358–1363.
[15] P. Obexer, K. Geiger, P.F. Ambros, B. Meister, M.J. Ausserlechner, FKHRL1-mediated expression of Noxa and Bim induces apoptosis via the mitochondria in neuroblastoma cells, Cell Death Differ. 14 (3) (2007) 534–547.
[16] P. Dey, A. Strom, J.A. Gustafsson, Estrogen receptor beta upregulates FOXO3a and causes induction of apoptosis through PUMA in prostate cancer, Oncogene 33 (33) (2014) 4213–4225.
[17] C.F. Chiu, Y.W. Chang, K.T. Kuo, Y.S. Shen, C.Y. Liu, Y.H. Yu, C.C. Cheng, K.Y. Lee, F.C. Chen, M.K. Hsu, T.C. Kuo, J.T. Ma, J.L. Su, NF-kappaB-driven suppression of FOXO3a contributes to EGFR mutation-independent gefitinib resistance, Proc. Natl. Acad. Sci. U. S. A. 113 (18) (2016) E2526–E2535.
[18] H. Liu, J. Yin, H. Wang, G. Jiang, M. Deng, G. Zhang, X. Bu, S. Cai, J. Du, Z. He, FOXO3a modulates WNT/beta-catenin signaling and suppresses epithelial-to-mesenchymal transition in prostate cancer cells, Cell. Signal. 27 (3) (2015) 510–518.
[19] E.C. Ferber, B. Peck, O. Delpuech, G.P. Bell, P. East, A. Schulze, FOXO3a regulates reactive oxygen metabolism by inhibiting mitochondrial gene expression, Cell Death Differ. 19 (6) (2012) 968–979.
[20] M. Wang, Y. Liu, J. Zou, R. Yang, F. Xuan, Y. Wang, N. Gao, H. Cui, Transcriptional co-activator TAZ sustains proliferation and tumorigenicity of neuroblastoma by targeting CTGF and PDGF-beta, Oncotarget 6 (11) (2015) 9517–9530.
[21] Z. Dong, Q. Lei, R. Yang, S. Zhu, X.X. Ke, L. Yang, H. Cui, L. Yi, Inhibition of neurotensin receptor 1 induces intrinsic apoptosis via let-7a-3p/Bcl-w axis in glioblastoma, Br. J. Cancer 116 (12) (2017) 1572–1584.
[22] R. Yang, L. Yi, Z. Dong, Q. Ouyang, J. Zhou, Y. Pang, Y. Wu, L. Xu, H. Cui, Tigecycline inhibits glioma growth by regulating miRNA-199b-5p-HES1-AKT pathway, Mol. Cancer Ther. 15 (3) (2016) 421–429.
[23] B.G. Hill, G.A. Benavides, J.R. Lancaster Jr., S. Ballinger, L. Dell'Italia, Z. Jianhua, V.M. Darley-Usmar, Integration of cellular bioenergetics with mitochondrial quality control and autophagy, Biol. Chem. 393 (12) (2012) 1485–1512.
[24] J. He, Y. Zhao, E. Zhao, X. Wang, Z. Dong, Y. Chen, L. Yang, H. Cui, Cancer-testis specific gene OIP5: a downstream gene of E2F1 that promotes tumorigenesis and metastasis in glioblastoma by stabilizing E2F1 signalling, Neuro-Oncol. 20 (9) (2018) 1173–1184.
[25] W. Deng, Y. Wang, Z. Liu, H. Cheng, Y. Xue, HemI: a toolkit for illustrating heatmaps, PLoS One 9 (11) (2014) e111988.
[26] F.E. Bleeker, N.A. Atai, S. Lamba, A. Jonker, D. Rijkeboer, K.S. Bosch, W. Tigchelaar, D. Troost, W.P. Vandertop, A. Bardelli, C.J. Van Noorden, The prognostic IDH1 (R132) mutation is associated with reduced NADP+-dependent IDH activity in glioblastoma, Acta Neuropathol. 119 (4) (2010) 487–494.
[27] V. Gleize, A. Alentorn, L. Connen de Kerillis, M. Labussiere, A.A. Nadaradjane, E. Mundwiller, C. Ottolenghi, S. Mangesius, A. Rahimian, F. Ducray, K. Mokhtari, C. Villa, M. Sanson, CIC inactivating mutations identify aggressive subset of 1p19q codeleted gliomas, Ann. Neurol. 78 (3) (2015) 355–374.
[28] C. Bettegowda, N. Agrawal, Y. Jiao, M. Sausen, L.D. Wood, R.H. Hruban, F.J. Rodriguez, D.P. Cahill, R. McLendon, G. Riggins, V.E. Velculescu, S.M. Oba-Shinjo, S.K.N. Marie, B. Vogelstein, D. Bigner, H. Yan, N. Papadopoulos, K.W. Kinzler, Mutations in CIC and FUBP1 contribute to human oligodendroglioma, Science (New York, N.Y.) 333 (6048) (2011) 1453–1455.
[29] M. Puputti, O. Tynninen, H. Sihto, T. Blom, H. Mäenpää, J. Isola, A. Paetau, H. Joensuu, N.N. Nupponen, Amplification of KIT, PDGFRA, VEGFR2, and EGFR in gliomas, Mol. Cancer Res. 4 (12) (2006) 927–934.
[30] D. Sturm, H. Witt, V. Hovestadt, D.-A. Khuong-Quang, David T.W. Jones, C. Konermann, E. Pfaff, M. Tönjes, M. Sill, S. Bender, M. Kool, M. Zapatka, N. Becker, M. Zucknick, T. Hielscher, X.-Y. Liu, Adam M. Fontebasso, M. Ryzhova, S. Albrecht, K. Jacob, M. Wolter, M. Ebinger, Martin U. Schuhmann, T. van Meter, Michael C. Frühwald, H. Hauch, A. Pekrun, B. Radlwimmer, T. Niehues, G. von Komorowski, M. Dürken, Andreas E. Kulozik, J. Madden, A. Donson, Nicholas K. Foreman, R. Drissi, M. Fouladi, W. Scheurlen, A. von Deimling, C. Monoranu, W. Roggendorf, C. Herold-Mende, A. Unterberg, Christof M. Kramm, J. Felsberg, C. Hartmann, B. Wiestler, W. Wick, T. Milde, O. Witt, Anders M. Lindroth, J. Schwartzentruber, D. Faury, A. Fleming, M. Zakrzewska, Pawel P. Liberski, K. Zakrzewski, P. Hauser, M. Garami, A. Klekner, L. Bognar, S. Morrissy, F. Cavalli, Michael D. Taylor, P. van Sluis, J. Koster, R. Versteeg, R. Volckmann, T. Mikkelsen, K. Aldape, G. Reifenberger, V.P. Collins, J. Majewski, A. Korshunov, P. Lichter, C. Plass, N. Jabado, Stefan M. Pfister, Hotspot mutations in H3F3A and IDH1 define distinct epigenetic and biological subgroups of glioblastoma, Cancer Cell 22 (4) (2012) 425–437.
[31] C.F. de Souza, T.S. Sabedot, T.M. Malta, L. Stetson, O. Morozova, A. Sokolov, P.W. Laird, M. Wiznerowicz, A. Iavarone, J. Snyder, A. deCarvalho, Z. Sanborn, K.L. McDonald, W.A. Friedman, D. Tirapelli, L. Poisson, T. Mikkelsen, C.G. Carlotti Jr., S. Kalkanis, J. Zenklusen, S.R. Salama, J.S. Barnholtz-Sloan, H. Noushmehr, A distinct DNA methylation shift in a subset of glioma CpG Island methylator phenotypes during tumor recurrence, Cell Rep. 23 (2) (2018) 637–651.
[32] M.E. Hegi, A.-C. Diserens, T. Gorlia, M.-F. Hamou, N. de Tribolet, M. Weller, J.M. Kros, J.A. Hainfellner, W. Mason, L. Mariani, J.E.C. Bromberg, P. Hau, R.O. Mirimanoff, J.G. Cairncross, R.C. Janzer, R. Stupp, MGMT gene silencing and benefit from temozolomide in glioblastoma, N. Engl. J. Med. 352 (10) (2005) 997–1003.
[33] C. Sebastian, B.M. Zwaans, D.M. Silberman, M. Gymrek, A. Goren, L. Zhong, O. Ram, J. Truelove, A.R. Guimaraes, D. Toiber, C. Cosentino, J.K. Greenson, A.I. MacDonald, L. McGlynn, F. Maxwell, J. Edwards, S. Giacosa, E. Guccione, R. Weissleder, B.E. Bernstein, A. Regev, P.G. Shiels, D.B. Lombard, R. Mostoslavsky, The histone deacetylase SIRT6 is a tumor suppressor that controls cancer metabolism, Cell 151 (6) (2012) 1185–1199.
[34] H.S. Kim, C. Xiao, R.H. Wang, T. Lahusen, X. Xu, A. Vassilopoulos, G. Vazquez-Ortiz, W.I. Jeong, O. Park, S.H. Ki, B. Gao, C.X. Deng, Hepatic-specific disruption of SIRT6 in mice results in fatty liver formation due to enhanced glycolysis and triglyceride synthesis, Cell Metab. 12 (3) (2010) 224–236.
[35] E.S. Polson, V.B. Kuchler, KHS101 disrupts energy metabolism in human glioblastoma cells and reduces tumor growth in mice, Sci. Transl. Med. 10 (454) (2018).
[36] J. Kriel, K. Muller-Nedebock, Coordinated autophagy modulation overcomes glioblastoma chemoresistance through disruption of mitochondrial bioenergetics, Sci. Rep. 8 (1) (2018) 10348.
[37] E. Poteet, G.R. Choudhury, A. Winters, W. Li, M.G. Ryou, R. Liu, L. Tang, A. Ghorpade, Y. Wen, F. Yuan, S.T. Keir, H. Yan, D.D. Bigner, J.W. Simpkins, S.H. Yang, Reversing the Warburg effect as a treatment for glioblastoma, J. Biol. Chem. 288 (13) (2013) 9153–9164.
[38] E.H. Kim, J.H. Lee, Y. Oh, I. Koh, J.K. Shim, J. Park, J. Choi, M. Yun, J.Y. Jeon, Y.M. Huh, J.H. Chang, S.H. Kim, K.S. Kim, J.H. Cheong, P. Kim, S.G. Kang, Inhibition of glioblastoma tumorspheres by combined treatment with 2-deoxyglucose and metformin, Neuro-oncology 19 (2) (2017) 197–207.
[39] H. Shen, E. Hau, S. Joshi, P.J. Dilda, K.L. McDonald, Sensitization of glioblastoma cells to irradiation by modulating the glucose metabolism, Mol. Cancer Ther. 14 (8) (2015) 1794–1804.
[40] M. Koukourakis, A. Tsolou, S. Pouliliou, I. Lamprou, M. Papadopoulou, M. Ilemosoglou, G. Kostoglou, D. Ananiadou, E. Sivridis, A. Giatromanolaki, Blocking LDHA glycolytic pathway sensitizes glioblastoma cells to radiation and temozolomide, Biochem. Biophys. Res. Commun. 491 (4) (2017) 932–938.
[41] S.P. Mathupala, Y.H. Ko, P.L. Pedersen, Hexokinase II: cancer's double-edged sword acting as both facilitator and gatekeeper of malignancy when bound to mitochondria, Oncogene 25 (34) (2006) 4777–4786.
[42] S.P. Mathupala, Y.H. Ko, P.L. Pedersen, Hexokinase-2 bound to mitochondria: cancer's stygian link to the "Warburg Effect" and a pivotal target for effective therapy, Semin. Cancer Biol. 19 (1) (2009) 17–24.
[43] L. Zhong, A. D'Urso, D. Toiber, C. Sebastian, R.E. Henry, D.D. Vadysirisack, A. Guimaraes, B. Marinelli, J.D. Wikstrom, T. Nir, C.B. Clish, B. Vaitheesvaran, O. Iliopoulos, I. Kurland, Y. Dor, R. Weissleder, O.S. Shirihai, L.W. Ellisen, J.M. Espinosa, R. Mostoslavsky, The histone deacetylase Sirt6 regulates glucose homeostasis via Hif1alpha, Cell 140 (2) (2010) 280–293.
[44] M. Choe, J.L. Brusgard, S. Chumsri, L. Bhandary, X.F. Zhao, S. Lu, O.G. Goloubeva, B.M. Polster, G.M. Fiskum, G.D. Girnun, M.S. Kim, A. Passaniti, The RUNX2 transcription factor negatively regulates SIRT6 expression to alter glucose metabolism in breast cancer cells, J. Cell. Biochem. 116 (10) (2015) 2210–2226.
[45] M. Wu, S.I. Dickinson, X. Wang, J. Zhang, Expression and function of SIRT6 in muscle invasive urothelial carcinoma of the bladder, Int. J. Clin. Exp. Pathol. 7 (10) (2014) 6504–6513.
[46] X.X. Feng, J. Luo, M. Liu, W. Yan, Z.Z. Zhou, Y.J. Xia, W. Tu, P.Y. Li, Z.H. Feng, D.A. Tian, Sirtuin 6 promotes transforming growth factor-beta1/H2O2/HOCl-mediated enhancement of hepatocellular carcinoma cell tumorigenicity by suppressing cellular senescence, Cancer Sci. 106 (5) (2015) 559–566.
[47] S. Khatri, H. Yepiskoposyan, C.A. Gallo, P. Tandon, D.R. Plas, FOXO3a regulates glycolysis via transcriptional control of tumor suppressor TSC1, J. Biol. Chem. 285 (21) (2010) 15960–15965.
[48] K.S. Jensen, T. Binderup, K.T. Jensen, I. Therkelsen, R. Borup, E. Nilsson, H. Multhaupt, C. Bouchard, B. Quistorff, A. Kjaer, G. Landberg, P. Staller, FoxO3A promotes metabolic adaptation to hypoxia by antagonizing Myc function, EMBO J. 30 (22) (2011) 4554–4570.
[49] M. Chang, L. Qiao, B. Li, J. Wang, G. Zhang, W. Shi, Z. Liu, N. Gu, Z. Di, X. Wang, Y. Tian, Suppression of SIRT6 by miR-33a facilitates tumor growth of glioma through apoptosis and oxidative stress resistance, Oncol. Rep. 38 (2) (2017) 1251–1258.
[50] J. Feng, P.F. Yan, H.Y. Zhao, F.C. Zhang, W.H. Zhao, M. Feng, SIRT6 suppresses

glioma cell growth via induction of apoptosis, inhibition of oxidative stress and suppression of JAK2/STAT3 signaling pathway activation, Oncol. Rep. 35 (3) (2016) 1395–1402.

[51] X. Chen, B. Hao, Y. Liu, D. Dai, G. Han, Y. Li, X. Wu, X. Zhou, Z. Yue, L. Wang, Y. Cao, J. Liu, The histone deacetylase SIRT6 suppresses the expression of the RNA-binding protein PCBP2 in glioma, Biochem. Biophys. Res. Commun. 446 (1) (2014) 364–369.

[52] X. Chen, D. Li, Y. Gao, Y. Cao, B. Hao, Histone deacetylase SIRT6 inhibits glioma cell growth through down-regulating NOTCH3 expression, Acta Biochim. Biophys. Sin. 50 (4) (2018) 417–424.